

# Improvements in ERBS Attitude Determination Without Gyros

N 9 3 5 2 4 7 1 0

D. Chu, J. Glickman, and E. Harvie  
COMPUTER SCIENCES CORPORATION (CSC)

134736  
1 10

## ABSTRACT

Previous papers have described the modification of the Earth Radiation Budget Satellite (ERBS) Attitude Determination System (ADS) to overcome the impact of onboard gyro degradation and failure on attitude ground support of the mission. Two approaches were taken: implementing a Kalman filter in place of the batch-least-squares attitude estimator to account for the propagation error produced by high-noise gyro data, and modeling the ERBS attitude dynamics to restore rate information in the case of gyro failure. Both of these methods had shortcomings. In practice, the filter attitude diverged without complete sensor observability; and accurate dynamics modeling required knowledge of disturbance torque parameters that had to be determined manually. These difficulties have been overcome by improved tuning of the filter and by incorporating dynamics parameter estimation into the ERBS ADS.

\* This work was supported by the National Aeronautics and Space Administration (NASA)/Goddard Space Flight Center (GSFC), Greenbelt, Maryland, Contract NAS 5-31500.

## 1. INTRODUCTION

During the past 2-1/2 years, considerable effort has been devoted to overcoming the impact of gyro degradation and failure in Flight Dynamics Facility ground support of the ERBS mission. The ERBS Fine Attitude Determination System (FADS) is a batch-least-squares algorithm designed to use gyro measurements of spacecraft motion for propagating one-orbit attitude histories, which are critical for ground support activities such as sensor bias determination. Fine Sun sensor data for computing accurate single-frame attitudes are typically available for only 20 percent of one orbit. Propagation is especially important for yaw, which is directly observable only with the Sun sensor. At present, four of six gyro channels have failed completely. Prior to each failure, there was an extended period (up to 16 months) when the accuracy of the gyro-propagated batch attitudes was degraded by high gyro noise. Reference 1 summarizes the ERBS gyro performance over the mission and the impact of gyro degradation on attitude determination accuracy.

Two approaches have been taken by the ERBS attitude support team to cope with the loss of accurate gyro data. Reference 2 describes the implementation of a Kalman filter recursive attitude estimation algorithm in the ERBS ADS to account for high gyro noise that caused up to 0.7-degree errors in standard batch attitudes. The filter was found to improve pitch and roll in the case of the high gyro noise, but yaw diverged due to incomplete sensor observability. To restore rate information when the gyros failed completely, attitude rates were modeled in the ADS and used for propagation in the standard batch FADS (References 3 and 4). Results of the dynamics modeling were good, but several torque parameters had to be determined manually—a time-consuming process that made operational use of the model impractical.

Continued efforts have improved the performance of both alternative attitude determination methods. This paper describes the improvements and evaluates the accuracy of each method.

## 2. ERBS BACKGROUND

The ERBS is a three-axis stabilized, Earth-oriented spacecraft, launched in 1984 into a near-circular orbit with an altitude of 600 km and an inclination of 57 degrees. Attitude is referenced to a geodetic coordinate system with pitch defined about negative orbit normal (y-axis), yaw about the local nadir vector (z-axis), and roll approximately along the velocity vector (x-axis). Attitude is controlled to plus or minus 1.0 degree on each axis. The control system used for normal flight consists of a pitch axis momentum wheel that maintains a strong angular momentum bias and controls pitch, two differentially driven horizon scanners mounted with their axes in the y-z plane to control yaw, and electromagnetic dipoles to control roll and manage pitch axis angular momentum. Requirements for ground attitude determination accuracy are 0.25 degree on each axis. This accuracy was to be achieved using gyros, horizon scanner measurements, and digital fine Sun sensor data, which are usually available for only 20 percent of one 97-minute orbit. At present, the pitch and roll channels of both redundant gyro packages have failed.

## 3. THE ERBS KALMAN FILTER

The software modifications to convert the batch FADS to a recursive Kalman filter are minimal, as many computations in the two algorithms are identical (Reference 2). In practice, the relative merits of each estimator must be considered when using them under different conditions. Batch algorithms offer robustness with respect to sensor error, but are strongly dependent on the accuracy of the propagation model. A recursive estimator is less dependent on the accuracy of the propagation model, but is sensitive to sensor error and difficult to tune. Gyro-based propagation in a batch estimator gives good results as long as the gyro data are accurate. However, there is a point at which propagation error degrades the accuracy of batch attitudes enough that, even with its limitations, the Kalman filter performs better.

One-orbit batch and filter attitudes are compared in Figures 1 through 6, where the time span is from a period in the mission when the gyro data were accurate and had low noise (0.003 deg/sec root-mean-square [RMS] standard deviation on each axis). The reference attitude is a single frame QUaternion ESTimator (QUEST) solution computed using fine Sun sensor data. Single-frame QUEST attitudes computed with fine Sun sensor data are accurate to within 0.05 degree for roll and yaw and are considered an absolute reference for those axes. Due to the close alignment of the pitch axis and Sun line for the full Sun sensor coverage geometry, the QUEST pitch solution is based mostly on horizon scanner data and is accurate only to within about 0.2 degree. To simulate typical sensor observability conditions in the batch and filter runs, 80 percent of the Sun sensor data have been manually flagged and are not used in the estimation process. The timespan is chosen so that Sun sensor coverage occurs at the beginning and end of the orbit. The filter pitch and roll (Figures 1 and 2) follow the sensor observations closely and remain within 0.3 degree of the reference QUEST pitch and roll. The filter yaw generally diverges when Sun sensor data are lost through the middle of the orbit. However, trial-and-error tuning can postpone divergence until Sun sensor data are reacquired (Figure 3). The batch attitude (Figures 4 through 6) diverges from the QUEST solution by up to 0.3 degree. Departures of the batch solution from the reference are attributed to a nonoptimal value of the epoch state, owing to the dependence on the less accurate horizon scanner data, and to a random walk in the gyro propagation that exists even for low-noise gyros.

Figures 7 through 12 show batch and filter comparisons from a period in the mission when the pitch and roll gyro noise was very high (0.012 deg/sec RMS). The batch pitch and roll (Figures 7 and 8) diverge by up to 0.7 degree. Pitch and roll propagation shows little correlation with real attitude motion. Even the batch yaw (Figure 9), with lower gyro noise (0.005 deg/sec RMS), is degraded through coupling of the large roll error into yaw. The Kalman filter (Figures 10 through 12) clearly performs better than the standard batch FADS in

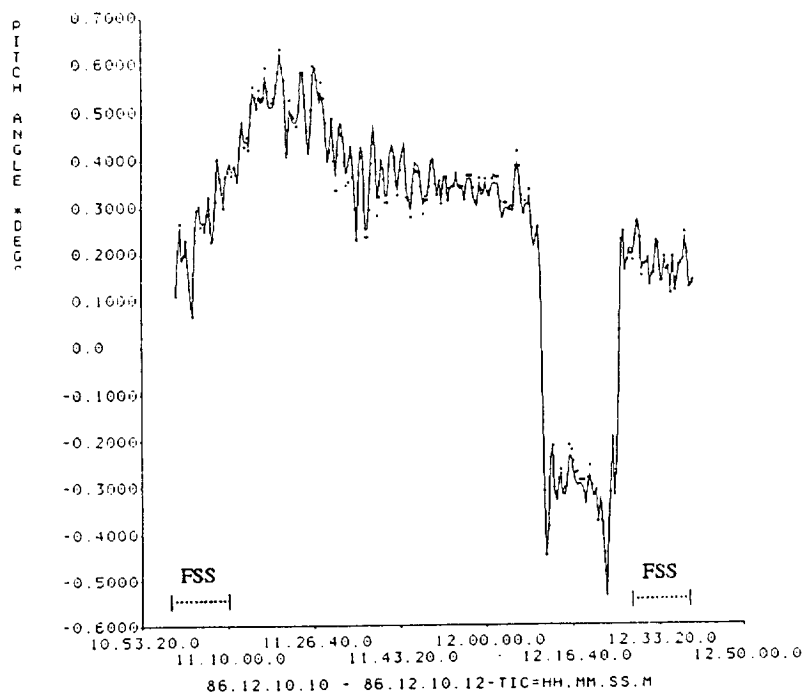


**Figure 1. One-orbit pitch comparisons for the filter solution using accurate gyro data for propagation (solid line) and the single frame QUEST reference solution (points) (Periods of fine Sun sensor data availability for this timespan are denoted by the dashed line.)**

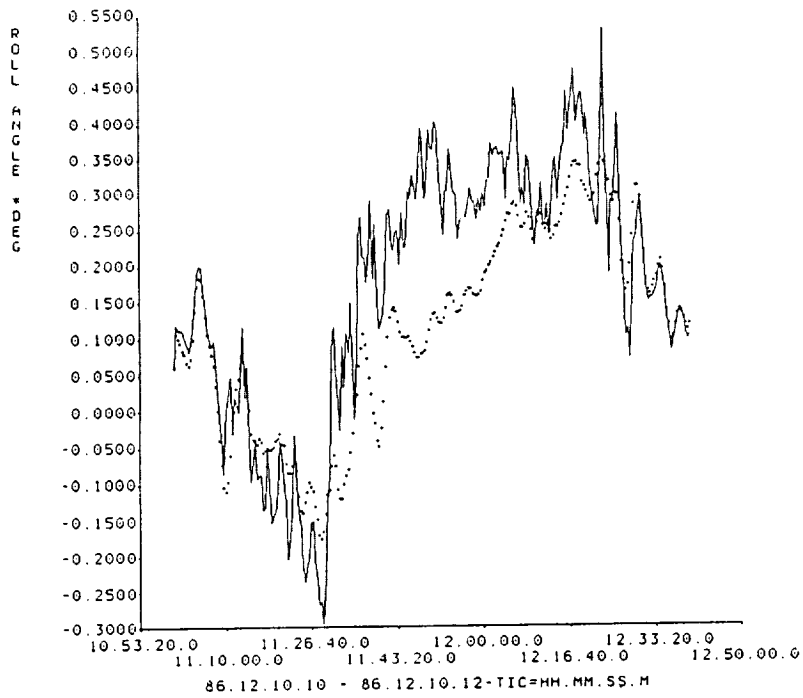


**Figure 2. One-orbit roll comparisons for the filter solution using accurate gyro data for propagation (solid line) and the single frame QUEST reference solution (points)**

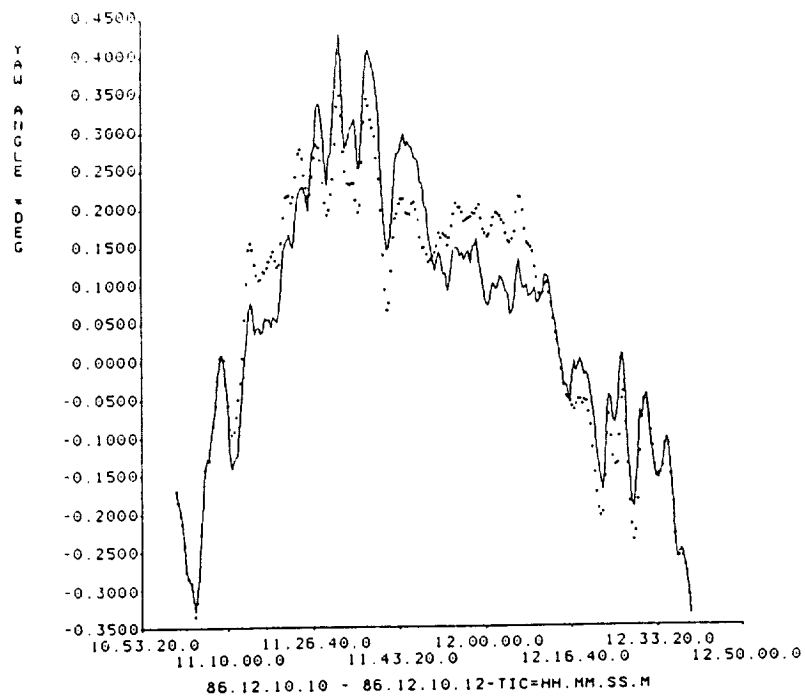


**Figure 3. One-orbit yaw comparisons for the filter solution using accurate gyro data for propagation (solid line) and the single frame QUEST reference solution (points)**

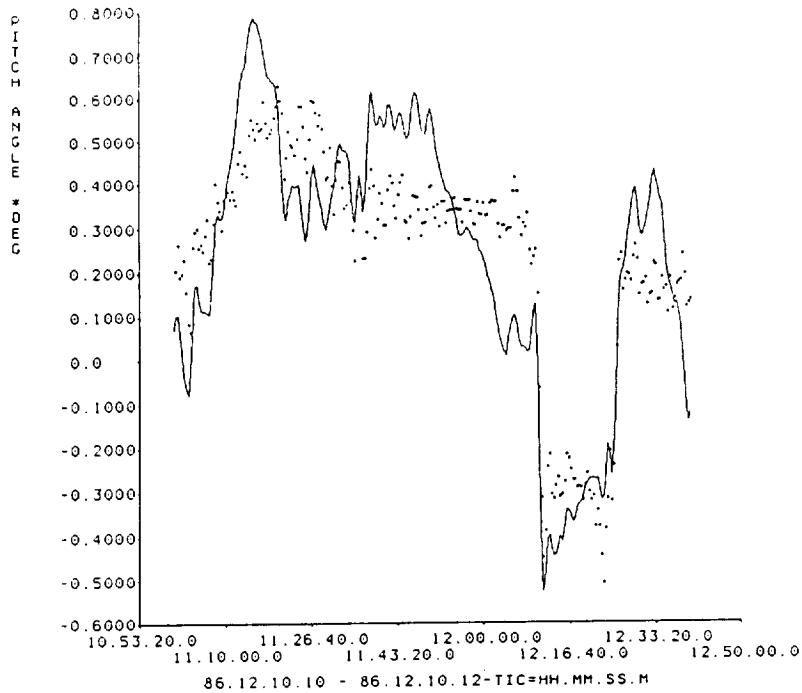


**Figure 4. One-orbit pitch comparisons for the batch solution using accurate gyro data for propagation (solid line) and the single frame QUEST reference solution (points)**

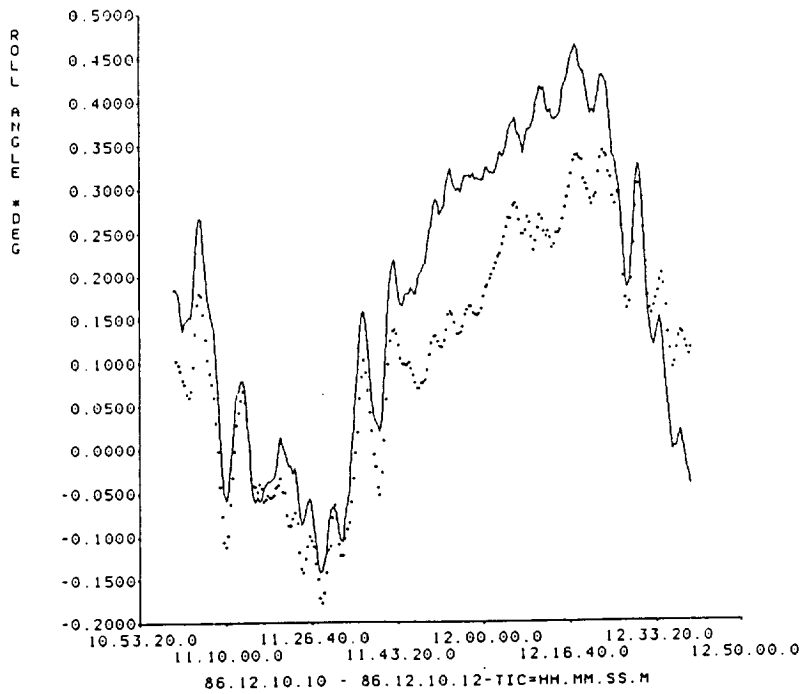


**Figure 5. One-orbit roll comparisons for the batch solution using accurate gyro data for propagation (solid line) and the single frame QUEST reference solution (points)**

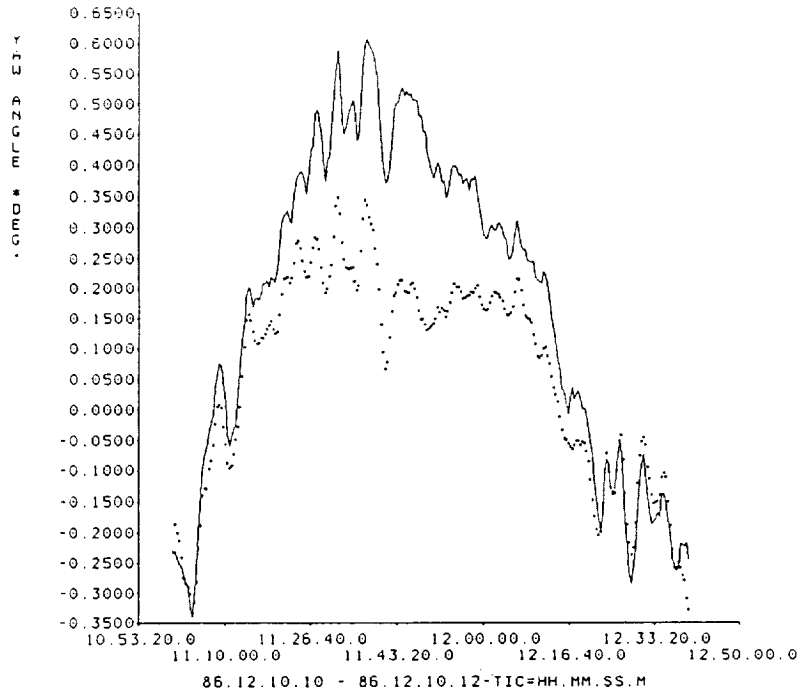


**Figure 6. One-orbit yaw comparisons for the batch solution using accurate gyro data for propagation (solid line) and the single frame QUEST reference solution (points)**

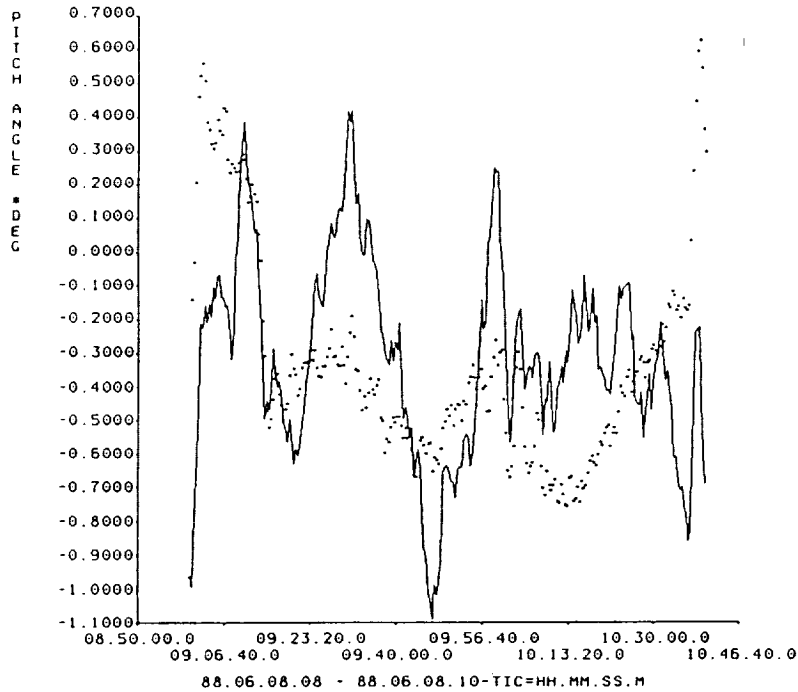


**Figure 7. One-orbit pitch comparisons for the batch solution using high noise gyro data for propagation (solid line) and the single frame QUEST reference solution (points) (Periods of fine Sun sensor data availability for this time span are denoted by the dashed line.)**

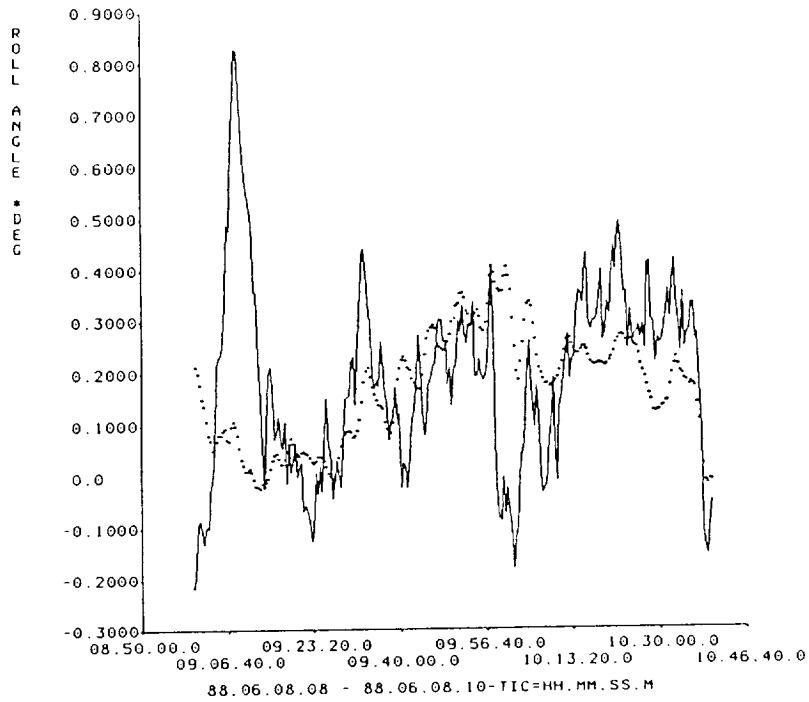


**Figure 8. One-orbit roll comparisons for the batch solution using high noise gyro data for propagation (solid line) and the single frame QUEST reference solution (points)**

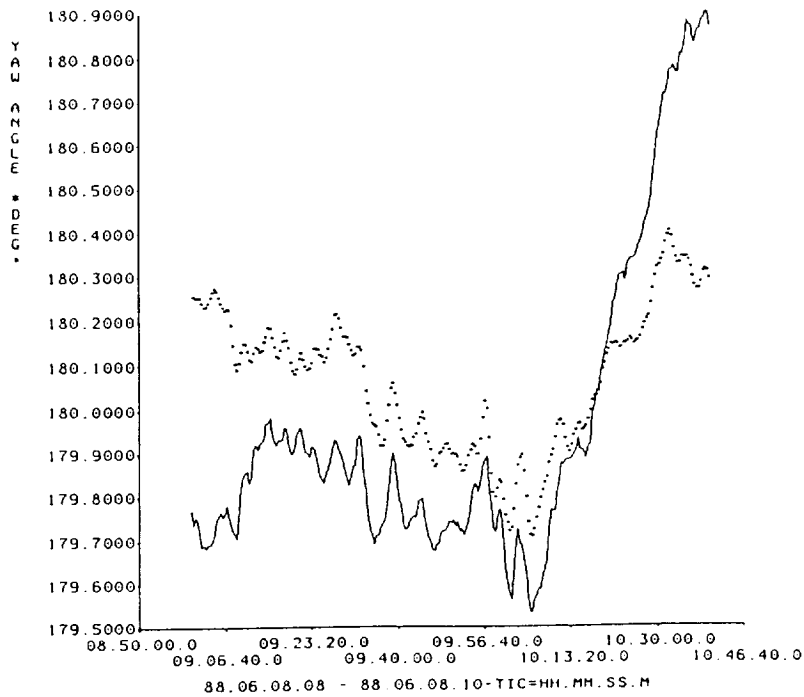


**Figure 9. One-orbit yaw comparisons for the batch solution using high noise gyro data for propagation (solid line) and the single frame QUEST reference solution (points)**

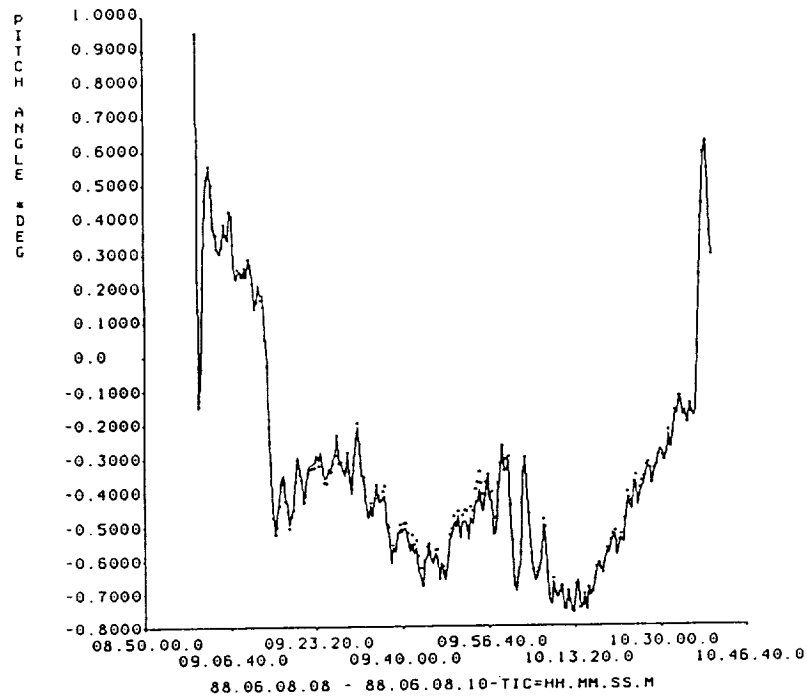


**Figure 10. One-orbit pitch comparisons for the filter solution using high noise gyro data for propagation (solid line) and the single frame QUEST reference solution (points)**

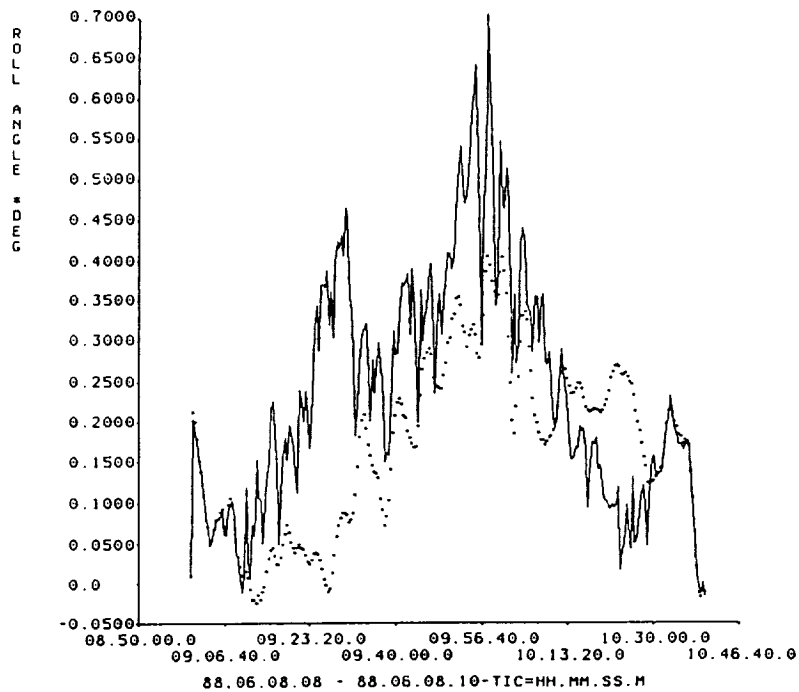


**Figure 11. One-orbit roll comparisons for the filter solution using high noise gyro data for propagation (solid line) and the single frame QUEST reference solution (points)**

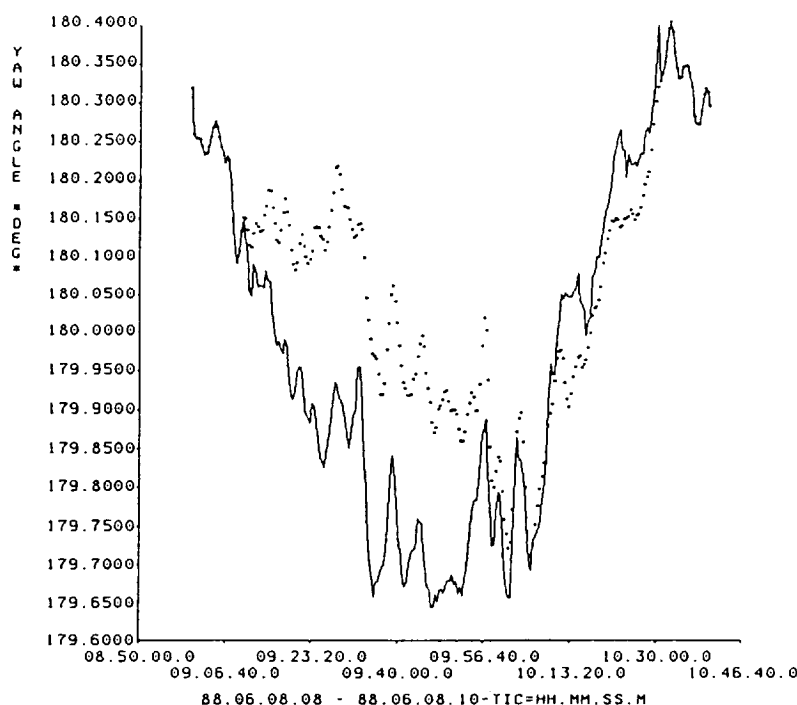


**Figure 12. One-orbit yaw comparisons for the filter solution using high noise gyro data for propagation (solid line) and the single frame QUEST reference solution (points)**

this example. However, the value of the process noise covariance matrix (the principal tuning parameter of the filter) that removes the divergence in yaw is inconsistent for different time spans. This difficulty may be overcome by determining different process noise terms for various levels of gyro noise, but it limits the usefulness of the filter for routine attitude determination.

#### 4. DYNAMICS ESTIMATION – BACKGROUND

An alternative to gyro propagation altogether has been implemented in ERBS attitude support (References 3 and 4). Euler's equation for rigid-body motion was solved for the angular velocity using spacecraft control system telemetry data for computing the control torques and mathematical models for computing the disturbance torques. Using these modeled rates for propagation in the standard batch FADS, matches to within 0.2 deg of accurate gyro-propagated solutions were obtained. However, modeled attitudes of this accuracy require the use of several uncertain parameters to compute the pitch axis disturbance torque. These parameters were identified as the spacecraft x-z product of inertia,  $I_{xz}$ , important in the pitch component of the gravity gradient torque; and the x and z residual dipole moments,  $m_x$  and  $m_z$ , important in the pitch axis magnetic disturbance torque. Values for these parameters were found to be inconsistent for different data spans and had to be determined manually for each run by trial and error.

To make routine use of the dynamics model practical, an automatic method of determining the uncertain torque parameters is necessary. The original batch FADS offers a convenient framework for estimating these parameters. The original FADS solves for a nine-dimension state vector consisting of the epoch attitude, gyro drift rate biases, and gyro scale factors. In the dynamics estimator, the three gyro scale factor state vector elements are replaced with the dynamics parameters  $I_{xz}$ ,  $m_x$ , and  $m_z$ . (Adding more state vector elements to the nine-dimension state would require extensive software modifications, and the gyro scale factor is not strictly applicable to the modeled rates anyway.) In the modified FADS, the epoch attitude estimation method

is unchanged; however, the epoch rate biases now correspond to the initial angular velocity in the integration of Euler's equation and are estimated slightly differently (a priori values for the three rates are taken as zero for roll and yaw, and the one-revolution-per-orbit rate for pitch). The only changes in the estimation are the partial derivatives of the attitude with respect to the new state parameters. To obtain a correct nonlinear solution of the dynamics parameters, the Euler solution is performed inside the FADS differential correction iteration loop (the new estimates of the torque parameters change the modeled rates for each iteration).

The following is a discussion of the modifications to the FADS estimation process. The partial derivatives of the current attitude error,  $\Delta\vec{a}$ , with respect to the state parameters (epoch attitude,  $\Delta\vec{a}_0$ , epoch angular velocity,  $\Delta\vec{\omega}_0$ , and  $\Delta\vec{p}$  comprising the dynamics parameters) are

$$\Delta\vec{a} = \begin{bmatrix} \frac{\partial\Delta\vec{a}}{\partial\Delta\vec{a}_0} & \frac{\partial\Delta\vec{a}}{\partial\Delta\vec{\omega}_0} & \frac{\partial\Delta\vec{a}}{\partial\Delta\vec{p}} \end{bmatrix} \begin{bmatrix} \Delta\vec{a}_0 \\ \Delta\vec{\omega}_0 \\ \Delta\vec{p} \end{bmatrix} \equiv F \begin{bmatrix} \Delta\vec{a}_0 \\ \Delta\vec{\omega}_0 \\ \Delta\vec{p} \end{bmatrix} \quad (1)$$

There are two linearized differential equations governing the propagation of attitude and angular velocity error.

$$\frac{d\Delta\vec{a}}{dt} = -\bar{\omega}\Delta\vec{a} + \Delta\vec{\omega} \quad (2)$$

$$\frac{d\Delta\vec{\omega}}{dt} = I^{-1}(\tilde{H}' - \bar{\omega}I)\Delta\vec{\omega} + I^{-1}\frac{\partial\Delta\vec{N}}{\partial\Delta\vec{p}}\Delta\vec{p} \quad (3)$$

The primed angular momentum  $\tilde{H}'$  is the total angular momentum, including both that of the body ( $I(\bar{\omega} + \Delta\vec{\omega})$ ) and the wheel  $\vec{h}$ . (The tilde denotes the antisymmetric matrix construction of a vector.)

$$\tilde{H}' = I(\bar{\omega} + \Delta\vec{\omega}) + \vec{h} \quad (4)$$

The vector  $\Delta\vec{N}$  is the error in the torque used to propagate the attitude. The columns of the torque derivative matrix are

$$\frac{\partial\Delta\vec{N}}{\partial\Delta I_{xz}} = \frac{3\mu}{r^3} (0 \ 1 \ -\text{roll})^T \equiv (0 \ \alpha \ -\beta)^T \quad (5)$$

$$\frac{\partial\Delta\vec{N}}{\partial\Delta m_x} = (0 \ -B_3 \ B_2)^T \quad (6)$$

$$\frac{\partial\Delta\vec{N}}{\partial\Delta m_z} = (-B_2 \ B_1 \ 0)^T \quad (7)$$

where  $\mu$  is the gravitational constant,  $r$  is the distance to the center of the Earth, and  $\vec{B}$  is the measured geomagnetic field in body coordinates.

The solutions to the attitude and angular velocity error equations have the following form

$$\Delta\vec{a}(t) = \phi(t)\Delta\vec{a}_0 + \psi(t)\Delta\vec{\omega}_0 \quad (8)$$

$$\Delta\vec{\omega}(t) = \xi(t)\Delta\vec{\omega}_0 + \gamma(t)\Delta\vec{p} \quad (9)$$

If the coefficient matrices can be considered constant over a short time, the state transition matrix ( $\phi$ ) is the matrix exponential of the coefficient matrix.

$$\phi = e^{-\bar{\omega}t} = \cos \omega t [1] + (1 - \cos \omega t) \frac{\omega \omega^T}{\|\omega\|^2} - \sin \omega t \frac{\bar{\omega}}{\|\omega\|} \quad (10)$$

The variational matrix ( $\Psi$ ) is the integral of the state transition matrix.

$$\psi(t) = \int_0^t \phi(\tau) d\tau = \frac{\sin \omega t}{\|\omega\|} [1] + (\cos \omega t - 1) \frac{\bar{\omega}}{\|\omega\|} - (\sin \omega t - \omega t) \frac{\omega \omega^T}{\|\omega\|^2} \quad (11)$$

Such closed-form expressions are not now available for the angular velocity error (equation 3). These will be approximated by the first few terms of the power series expansion for the matrix exponential

$$e^{At} = [1] + At + \frac{1}{2} A^2 t^2 + \frac{1}{3!} A^3 t^3 + \dots \quad (12)$$

where

$$A = I^{-1}(\tilde{H}' - \bar{\omega}I) \quad (13)$$

Over long time spans, when the coefficient matrices may not be constant, these equations can be solved recursively. The closed-form expressions and truncated series approximations above can be used over the short individual time steps to update the previous solution values.

$$\Delta \vec{a}_i = \phi_i \Delta \vec{a}_{i-1} + \psi_i \Delta \vec{\omega}_i \quad (14)$$

$$\Delta \vec{\omega}_i = \xi(\tau)_i \Delta \vec{\omega}_{i-1} + \gamma_i \Delta \vec{p} \quad (15)$$

where

$$\xi_i = e^{A_i t} \quad (16)$$

and

$$\gamma_i = \int_{t_i}^{t_i + \Delta t} \xi(\tau) I^{-1} \frac{\partial \Delta \vec{N}_i}{\partial \Delta \vec{p}} d\tau \quad (17)$$

If the partial derivative of the torque with respect to the dynamics parameters is almost constant over the short time step, it can be brought outside of the integral. This last expression then can be approximated as follows:

$$\gamma_i \approx A_i^{-1} (e^{A_i \Delta t} - [1]) I^{-1} \begin{bmatrix} 0 & 0 & -B_2 \\ \alpha & -B_3 & B_1 \\ -\beta & B_2 & 0 \end{bmatrix} \quad (18)$$

The accumulated matrix for the attitude error is

$$\frac{\partial \Delta \vec{a}_i}{\partial \Delta \vec{a}_0} = \phi_i \phi_{i-1} \phi_{i-2} \dots \phi_2 \phi_1 \equiv \Phi_i \quad (19)$$

The accumulated matrix for the angular velocity error is

$$\frac{\partial \Delta \vec{a}_i}{\partial \Delta \vec{\omega}_0} = \phi_i \frac{\partial \Delta \vec{a}_{i-1}}{\partial \Delta \vec{\omega}_0} + \frac{\partial \Delta \vec{a}_i}{\partial \Delta \vec{\omega}_i} \frac{\partial \Delta \vec{\omega}_i}{\partial \Delta \vec{\omega}_0} = \phi_i \frac{\partial \Delta \vec{a}_{i-1}}{\partial \Delta \vec{\omega}_0} + \psi_i \Xi_i \quad (20)$$

where

$$\frac{\partial \Delta \vec{a}_0}{\partial \Delta \vec{\omega}_0} = [0] \quad (21)$$

$$\Xi_i = \xi_i \xi_{i-1} \xi_{i-2} \dots \xi_2 \xi_1 \quad (22)$$

The accumulated matrix for the product of inertia and residual dipole moments is

$$\frac{\partial \Delta \vec{a}_i}{\partial \Delta \vec{p}} = \phi_i \frac{\partial \Delta \vec{a}_{i-1}}{\partial \Delta \vec{p}} + \frac{\partial \Delta \vec{a}_i}{\partial \Delta \vec{\omega}_i} \frac{\partial \Delta \vec{\omega}_i}{\partial \Delta \vec{p}} = \phi_i \frac{\partial \Delta \vec{a}_{i-1}}{\partial \Delta \vec{p}} + \psi_i \Gamma_i \quad (23)$$

$\Gamma_i$  is computed recursively as follows:

$$\Gamma_i = \xi_i \Gamma_{i-1} + \gamma_i \quad (24)$$

where

$$\Gamma_0 = [0] \quad (25)$$

Combining these results, the partial derivative matrix of current attitude error with respect to the epoch attitude and angular velocity errors and dynamics parameters can be computed

$$F_i = \phi_i F_{i-1} + \psi_i [ 0 \mid \Xi_i \mid \Gamma_i ] \quad (26)$$

where

$$F_0 = \left\{ [1] \mid [0] \mid [0] \right\} \quad (27)$$

## 5. DYNAMICS ESTIMATION – RESULTS

To evaluate the performance of the ERBS dynamics estimation algorithm, pitch attitudes computed using the manual trial and error method and the dynamics estimator are compared with the gyro-propagated reference pitch. Figure 13 shows the modeled-to-reference pitch attitude history with the manually determined values of  $I_{xz}$ ,  $m_x$ , and  $m_z$ . With the manual variation of parameters method, approximately 12 runs of the Euler solution and FADS subsystem by an experienced analyst and about 2 hours of wall clock time were required to achieve a match of about 0.2 degree to the reference pitch. The modeled-to-reference pitch for the dynamics estimation is shown in Figure 14. Automatic estimation of the dynamics parameters was accomplished in five differential correction iterations and in a wall clock time of only 5 minutes. Table 1 gives the values of the parameters for each run, together with the RMS standard deviation of the fit to reference pitch and the weighted observation residuals. Not only does the automatic estimation greatly increase the efficiency of the dynamics determination process, but it also results in a better fit to the sensor measurements than was accomplished manually. Roll and yaw from the dynamics estimator solution, shown in Figures 15 and 16, match the gyro reference to within 0.1 degree RMS.

It is possible that the improvement in modeled pitch is due to the increased degrees of freedom in estimating the pitch axis disturbance torque and that the actual perturbations may be other than those modeled as gravity gradient and magnetic. However, these two disturbance torques are expected to be dominant for pitch.

Knowledge of the dynamics parameters may also be used to improve the onboard control system performance. For example, a momentum wheel bias voltage could be uplinked to offset the constant gravity gradient pitch torque from the non-zero  $I_{xz}$  inertia product, or a dipole bias could be uplinked to offset torques produced by the residual magnetic dipole moment if consistent values were observed. Trend analysis of the dynamics parameters is also possible. Table 2 shows estimated values of  $I_{xz}$ ,  $m_x$ , and  $m_z$  from recent mission data.

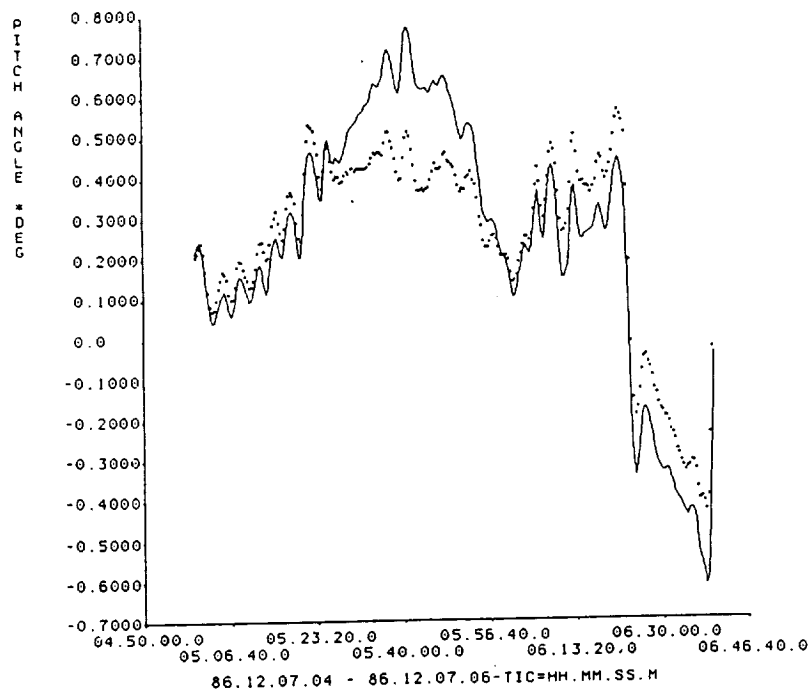


Figure 13. One-orbit pitch solution using modeled rates for propagation and manually determined disturbance torque parameters (solid line) and gyro-propagated reference (points)

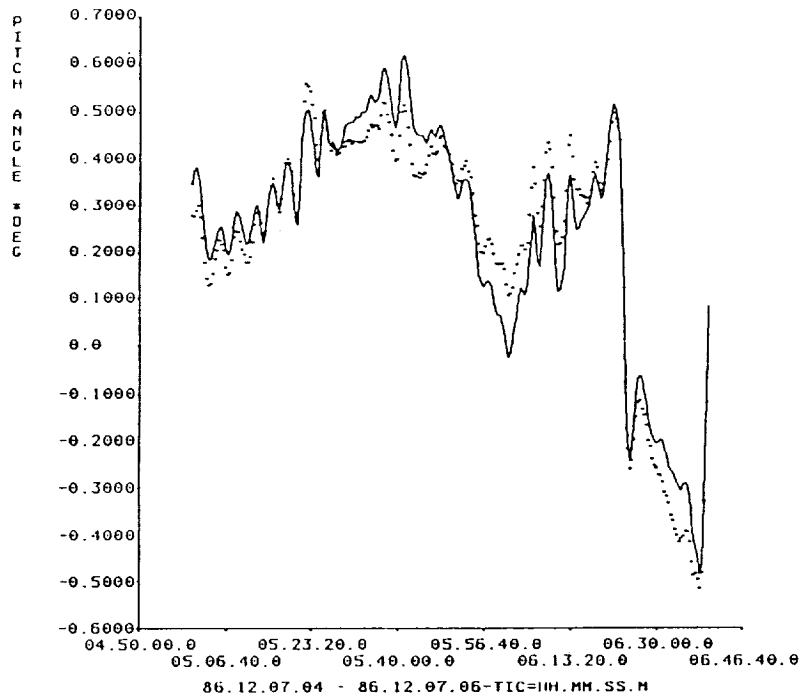


Figure 14. One-orbit pitch solution using modeled rates and automatically determined disturbance torque parameters (solid line) and gyro-propagated reference (points)

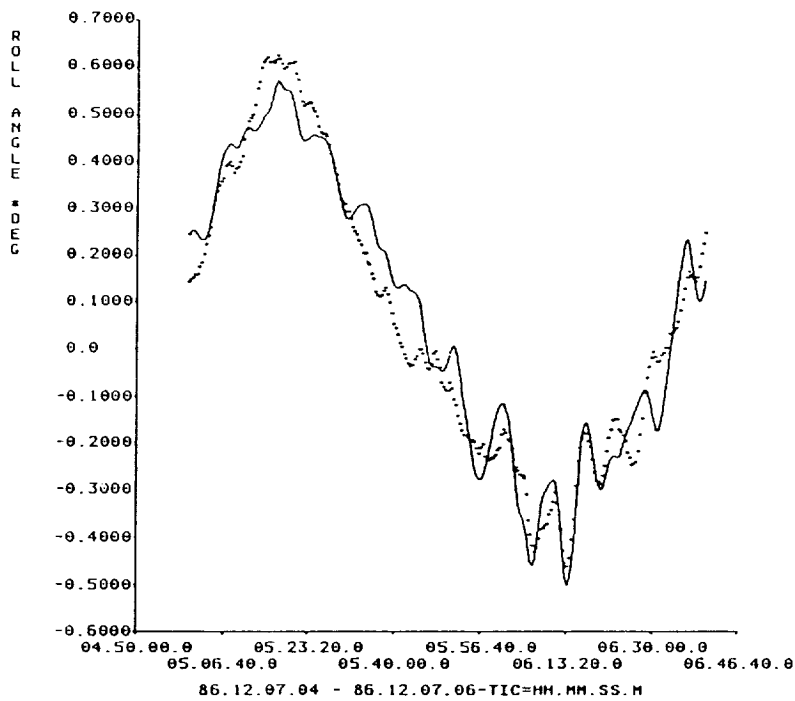


Figure 15. One-orbit roll solution using modeled rates and automatically determined disturbance torque parameters (solid line) and gyro-propagated reference (points)

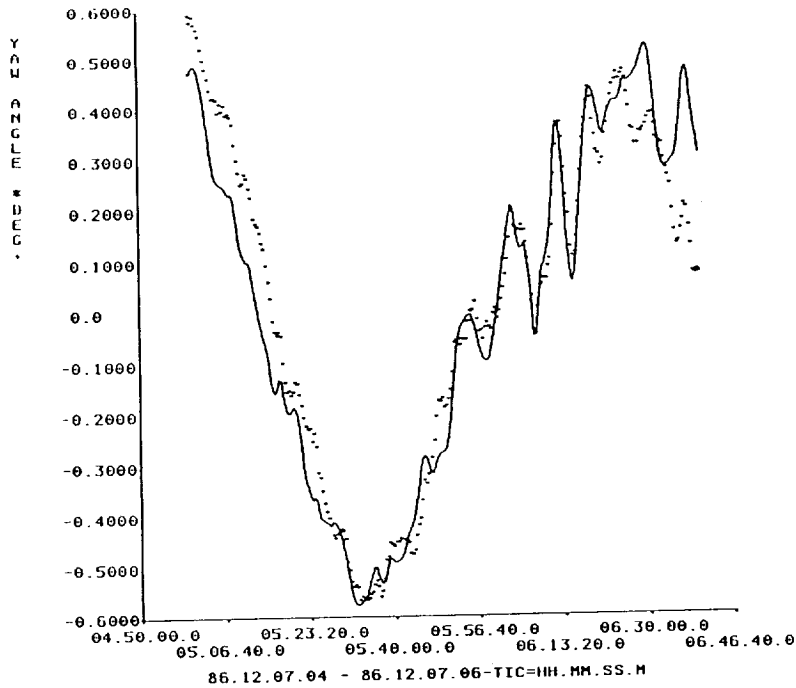


Figure 16. One-orbit yaw solution using modeled rates and automatically determined disturbance torque parameters (solid line) and gyro-propagated reference (points)

Table 1. Dynamics Estimation Comparisons for 861207

METHOD	$I_{xz}$ (kg-m <sup>2</sup> )	$m_x$ (ATm <sup>2</sup> )	$m_z$ (ATm <sup>2</sup> )	FIT TO REFERENCE PITCH (RMS)	WEIGHTED OBSERVATION RESIDUALS (RMS)
MANUAL	-20.00	3.50	0.50	0.12	0.901
DYNAMICS ESTIMATOR	-20.47	3.02	0.26	0.06	0.816
GYRO REFERENCE	-	-	-	-	0.776

Table 2. Dynamics Parameter Trends

DATE	$I_{xz}$ (kg-m <sup>2</sup> )	$m_x$ (ATm <sup>2</sup> )	$m_z$ (ATm <sup>2</sup> )	RESIDUALS (RMS)
920311	-42.6	1.71	-2.26	0.91
920320	-48.5	-0.51	1.03	1.21
920325	-52.1	0.42	2.05	1.35
920401	-42.8	0.93	2.64	1.13

## 6. CONCLUSIONS

Two strategies to overcome the loss of accurate gyro data in ground attitude determination support of the ERBS mission have been implemented. Both methods involve a modification of the existing ADS, taking advantage of existing software to minimize development effort.

Although the Kalman filter performs better than the batch estimator for very high gyro noise, the filter yaw solution is very sensitive to the process noise. Divergence in the filter yaw may be reduced by appropriate tuning of the process noise terms, but the tuning was found to be inconsistent even for time spans with the same gyro noise levels. This inconsistency in yaw behavior makes routine use of the filter impractical. An adaptive Kalman filter that determines the process noise automatically would be more suitable for the application to ERBS attitude determination, where the propagation noise has varied widely over the course of the mission.

The dynamics estimator is a viable solution to the problem of gyro failure for ERBS attitude ground support. Modeled rates can be used to propagate one-orbit attitudes to an accuracy within the 0.25-degree requirement with no a priori knowledge of disturbance torque parameters. Values of the dynamics parameters determined in the estimation process are also useful for analysis of control system performance. The dynamics estimator is currently being evaluated for operational use to restore full Flight Dynamics Facility attitude ground support of the ERBS mission.

## REFERENCES

1. Computer Sciences Corporation, 553-FDD-91/025R0UD0 (CSC/TM-91/6080R0UD0), *Earth Radiation Budget Satellite (ERBS) Inertial Reference Unit (IRU) Performance Analysis*, E. Harvie, J. Glickman, and K. Tran, February 1992
2. D. Chu and E. Harvie, *Accuracy of the ERBS Definitive Attitude Determination System in the Presence of Propagation Noise*, Flight Mechanics/Estimation Theory Symposium, NASA—Goddard Space Flight Center, May 1990
3. E. Harvie, D. Chu, and M. Woodard, *The Accuracy of Dynamic Attitude Propagation*, Flight Mechanics/Estimation Theory Symposium, NASA—Goddard Space Flight Center, May 1990
4. E. Harvie and D. Chu, *Dynamics Modeling for ERBS Attitude Propagation*, Third International Symposium on Spacecraft Flight Dynamics, Darmstadt, Germany, October 1991